# Evaluation of Fitting Parameters for Fat Fraction Estimation with MRI

**G. A. Flores*, Y. A. Costa**, E. L. L. Rodrigues**, F. F. Paiva***

*São Carlos Institute of Physics, University of São Paulo, São Carlos, Brazil

**Department of Electrical and Computer Engineering, University of São Paulo, São Carlos, Brazil

e-mail: gabriela.flores@usp.br

**Abstract** - *Hepatic Steatosis is the presence of fat in liver tissue, a pathology found in more than 30% of the US population. Magnetic resonance imaging is a reliable and reproducible exam for the assessment of liver fat fraction. This work analyzed the behavior of the standard fitting algorithm used in literature to estimate liver fat fraction with magnitude in-phase and opposed-phase images by varying a set of initial fitting parameters. The results led to a suggestion for optimal values.*

**Keywords**: *Fitting parameters, fat fraction, Levenberg-Marquadt, MRI*

## Introduction

Hepatic Steatosis is the presence of fat in liver tissue, a pathological condition found in more than 30% of US population [1] which is increasingly being diagnosed using magnetic resonance imaging (MRI) due to its reproducibility [2] and concordance to histologic data [3]. The amount of fat relative to that of water, namely fat fraction (FF), is estimated using gradient-recalled echo (GRE) images. These images are acquired at two echo times (TE) at which the signals from fat and water protons are presumed to be summed, forming in-phase (IP) images, or subtracted, in the opposed-phase (OP) images [4]. Current estimation methods are performed using nonlinear least squares to fit the signal from the image to a reduced version of the GRE equation and obtain FF.

It is known that the initialization parameters in a nonlinear fitting interfere directly on data estimation and convergence, and the most common algorithm used to search for the parameters is Levenberg–Marquardt. This work verified the error in FF estimation when varying initial parameters, searching for a set of general initialization values that would safely lead to convergence.

## Materials e Methods

Fat fraction is currently estimated by using variations of equation that describes the GRE signal and fitting the image data to them. The equation is generally simplified for low flip angles [5], for $n$ moieties precessing at different frequencies and results in the signal at a given TE:

$$S(TE) = |k\alpha \sum_n \rho_n \exp(\frac{-TE}{T2^*}) \exp(2\pi f_n TE)| \tag{1}$$

where k is a machine-specific proportionality constant, $\alpha$ is the flip angle, and $f_n$ is the precession frequency of the moiety. Fat fraction is defined as the relation between proton density of fat ($\rho_{fat}$) and the proton density of the total volume observed ($\rho_{total}$), which is considered to be made up of fat and water ($\rho_{water}$):

$$FF = \frac{\rho_{fat}}{\rho_{total}} \tag{2}$$

where $\rho_{total} = \rho_{water} + \rho_{fat}$. Signals from voxels from the IP/OP images are fitted by equation (1) in order to obtain $\rho_{water}$, $\rho_{fat}$ and subsequently FF.

The proposed work was implemented in Python 3 using Jupyter Notebook and Scipy packages. The GRE signal was simulated based on equation (1) for 7 TEs, considering a magnetic field of 3T, 6 fat components and 1 water component as suggested by Hamilton et al. [6]. Several simulations of the GRE signal were performed for different values of FF and results were fitted back to the equation using a range of initialization parameters ($\rho_{water}$ and $\rho_{fat}$). GRE signals were simulated for fat fractions ranging from 1 to 50% and their equivalent proton densities according to equation (2), considering $\rho_{total}$ as 10, 100 and 1000. In the fitting stage, for each FF value, the initialization value for either $\rho_{water}$ or $\rho_{fat}$ was fixed as matching to the corresponding value used to generate the signal, while the other parameter in its turn swept a range between 0 and $2 * \rho_{total}$ of the simulated sample. All tests were repeated adding Rician noise to the generated signal, with SNR values of 5, 10 and 20.

## Results

Figures 1-4 were generated considering $\rho_{total} = 1000$ even though the tests were repeated and consistent for other values (data not shown). The abscissas show the differences between the fixed and the variable proton density, either $\rho_{fat}$ or $\rho_{water}$. The ordinates show the differences between the estimated and the simulated (true) fat fraction, or error in estimation. Each simulation was repeated for ten different fat fractions and plotted altogether.

Figure 1A displays the results for the simulation without noise when the initial values passed to the fitting algorithm were matching the simulated ones for $\rho_{water}$ while $\rho_{fat}$ varies across the whole range. For small values, the algorithm converges to a local minimum, and this region of change in convergence can be better seen in Figure 1B. The same test is repeated for changes in $\rho_{water}$ while passing correct initial values for $\rho_{fat}$ in Figure 2, which now depicts a noticeable change in the acceptable difference between the initialization of the proton densities for each fat fraction. Figures 1C and 2C explore the effects of added noise for both variables in the change of results due to the increasing difference between $\rho_{fat}$ and $\rho_{water}$. Finally, figures 3 and 4 show the effects in the baseline results for different values of SNR.

## Discussion

When varying initialization values for $\rho_{fat}$ while keeping $\rho_{water}$ fixed matching the correct value, the algorithm admitted deviations in $\rho_{fat}$, estimating correct FF values as can be seen in Figure 1. When the difference $\rho_{water} - \rho_{fat}$ becomes larger than -17.6 for 39% FF and respective values for other fat fractions as shown in Figure 1B, the algorithm converges to a local minimum. Figure 1 also shows that for larger values of fat fractions, the algorithm tends to allow a smaller difference between the water and fat proton density. When initialized values for $\rho_{water}$ are varied while keeping $\rho_{fat}$ fixed as matching the correct value, the algorithm converged to a local minimum right after $\rho_{water}$ became smaller than $\rho_{fat}$ (i.e., $\rho_{varied} - \rho_{water} < 0$) as can be observed in Figure 2A. This result indicates that for these cases the algorithm is much more instable if the initial estimation of $\rho_{fat}$ is greater than $\rho_{water}$. The results are different due to how these variables affect Equation (1).

Adding noise to the signal, the local minimum behavior did not change for either case of initialization values, as can be seen in Figures 3 and 4. Figure 3 shows the results while changing $\rho_{fat}$ and Figure 4 for changes in $\rho_{water}$ for different SNRs, stressing that the fitting converges to the same local minima and maxima, slightly altered by the presence of noise. Even though for each iteration it was used a different random noise, the convergence leads to the same results. A general recommendation with the purpose of minimizing errors due to initialization can be derived from these results. Presuming that water molecules predominate in human liver and that the signal in a IP image is proportional to the sum of the signals from fat and water proton densities, we suggest the fitting initialization parameters to be $\rho_{water} = S(IP)/2$ and $\rho_{fat} < S(IP)/2$, where $S(IP)$ is the signal intensity of a voxel or region of interest located on the first IP image. This should guarantee convergence as the values are necessarily smaller than the real ones due to the signal decay and the relation between $\rho_{water}$ and $\rho_{fat}$ represents what it should be found in a real system evaluated by magnitude images.

## Conclusion

In this paper we analyzed the Levenberg–Marquard fitting algorithm in terms of its response according to the input initial values $\rho_{water}$ and $\rho_{fat}$ for the calculation of fat fraction according to the general gradient echo equation for small flip angles. The fitting method showed good response when varying the initial values of fitting, even when noise was inserted on GRE signal, as long as $\rho_{water} \geq \rho_{fat}$. The results led to a general recommendation for the initialization of the fitting algorithm when considering those variables in such a way that each should take the half of the value of the signal intensity of the voxel or region of interest in the first in-phase image.

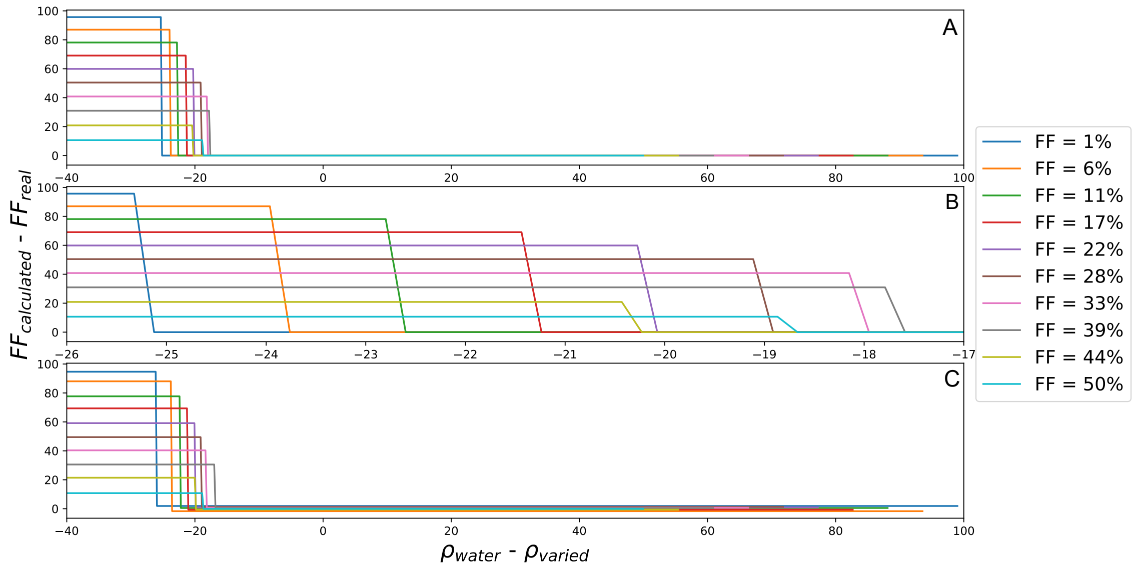


Figure 1 – Variation in $\rho_{fat}$ while $\rho_{water}$ is fixed for different values of FF. 1A has no noise on the signal, 1B is the zoomed area from 1A, 1C has an SNR = 20.

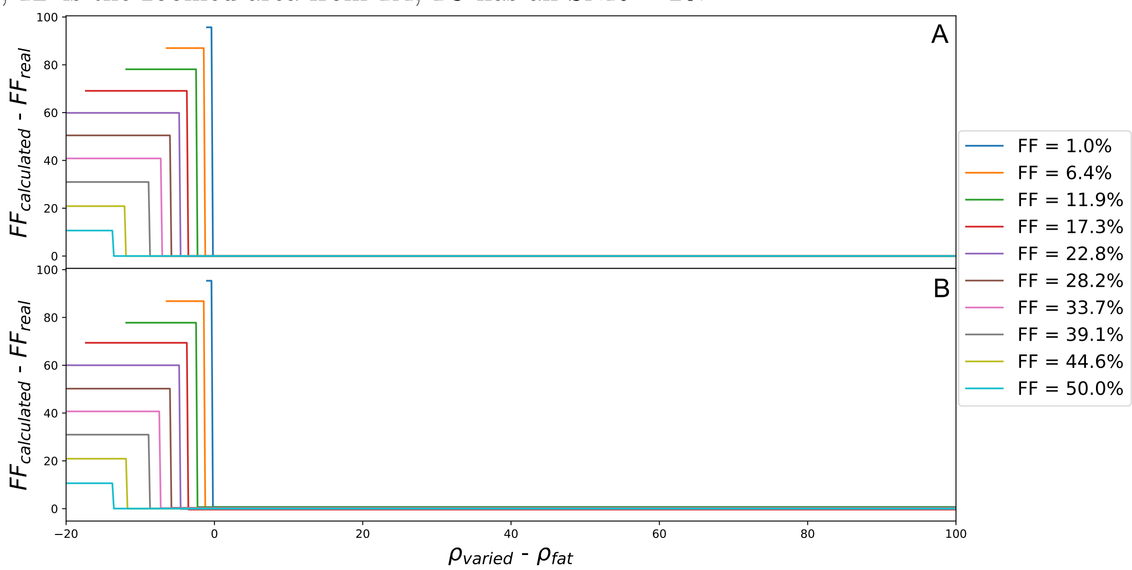


Figure 2 – Variation in $\rho_{water}$ while $\rho_{fat}$ is fixed for different values of FF. 2A has no noise on signal, 2B has an SNR = 20.

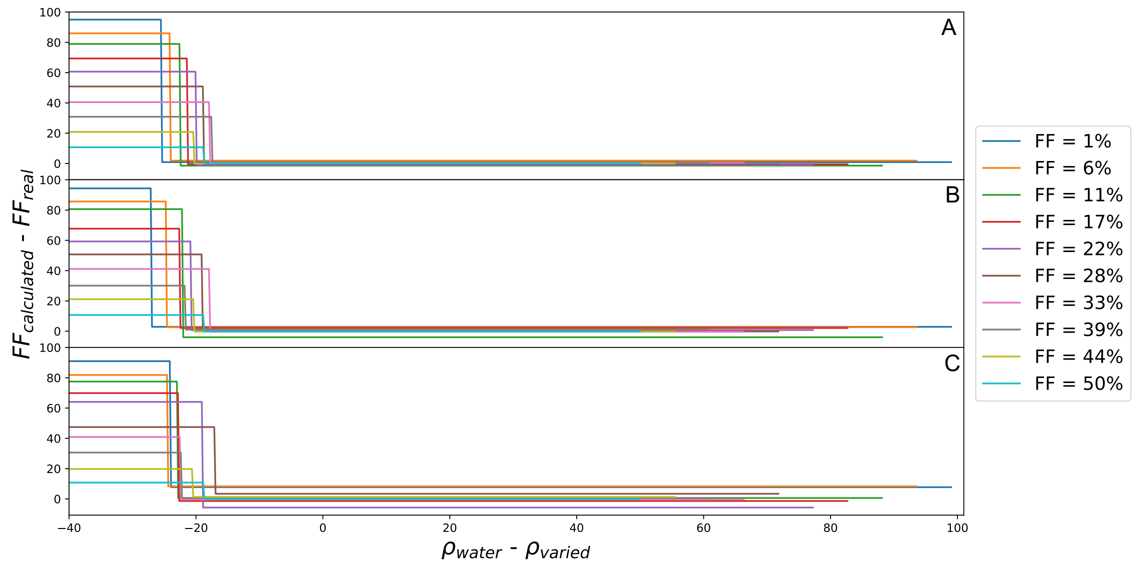


Figure 3 – Noise Variation when $\rho_{fat}$ is varied while $\rho_{water}$ is fixed for different values of FF. 3A has an SNR = 5, 3B has an SNR = 10, 3C has an SNR = 20

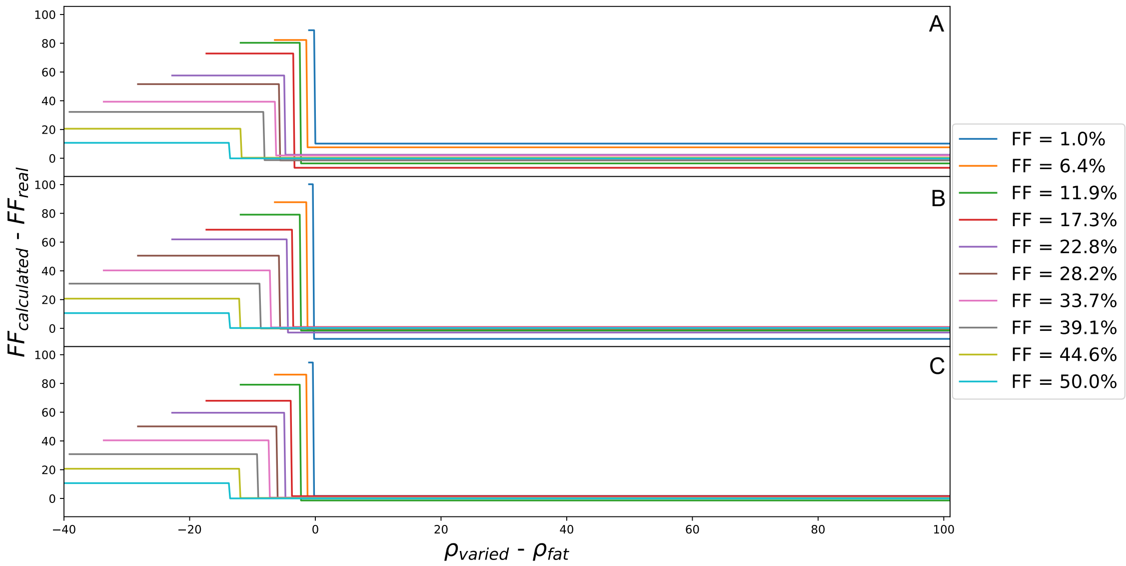


Figure 4 – Noise variation when $\rho_{water}$ is varied while $\rho_{fat}$ is fixed for different FF. 4A has an SNR = 5, 4B has an SNR = 10, 4C has an SNR = 20.

## References

[1] J. D. Browning, L. S. Szczepaniak, R. Dobbins, P. Nuremberg, J. D. Horton, J. C. Cohen, S. M. Grundy, and H. H. Hobbs, "Prevalence of hepatic steatosis in an urban population in the United States: Impact of ethnicity," *Hepatology*, vol. 40, pp. 1387–1395, 12 2004.

[2] G. H. Kang, I. Cruite, M. Shiehmorteza, T. Wolfson, A. C. Gamst, G. Hamilton, M. Bydder, M. S. Middleton, and C. B. Sirlin, "Reproducibility of MRI-determined proton density fat fraction across two different MR scanner platforms," *Journal of Magnetic Resonance Imaging*, vol. 34, pp. 928–934, 10 2011.

[3] S. M. Noworolski, M. M. Lam, R. B. Merriman, L. Ferrell, and A. Qayyum, "Liver steatosis: concordance of MR imaging and MR spectroscopic data with histologic grade.," *Radiology*, vol. 264, pp. 88–96, 7 2012.

[4] W. T. Dixon, "Simple proton spectroscopic imaging.," *Radiology*, vol. 153, pp. 189–194, 10 1984.

[5] T. Yokoo, M. Bydder, G. Hamilton, M. S. Middleton, A. C. Gamst, T. Wolfson, T. Hassanein, H. M. Patton, J. E. Lavine, J. B. Schwimmer, and C. B. Sirlin, "Nonalcoholic Fatty Liver Disease: Diagnostic and Fat-Grading Accuracy of Low-Flip-Angle Multiecho Gradient-Recalled-Echo MR Imaging at 1.5 T," *Radiology*, vol. 251, pp. 67–76, 4 2009.

[6] G. Hamilton, T. Yokoo, M. Bydder, I. Cruite, M. E. Schroeder, C. B. Sirlin, and M. S. Middleton, "In vivo characterization of the liver fat 1H MR spectrum," *NMR in Biomedicine*, vol. 24, pp. 784–790, 8 2011.